18

Measuring Dynamic Cell Volume In Situ by Confocal Microscopy

Rachel J. Errington and Nick S. White

1. Introduction

Regulation of cell volume is a fundamental homeostatic mechanism in the face of osmotic stress ***(1,2)***. One approach to understanding aspects of cell volume regulation involves the removal of cells from the matrix and manipulation in culture ***(3)***. Measurements are often also needed from cells within intact tissue that are operating in their correct physiological context. These include the effects of cell-cell interactions and the mechanical, ionic, and physiological effects of the extracellular matrix (ECM). The procedure described here is an *in situ* approach to volume measurement using an organ culture system, which maintains tissue integrity and hence the spatial organisation of cells in the ECM ***(4)***. We present a comprehensive protocol for investigating volume regulatory behaviour using confocal laser scanning microscopy (CLSM). Although we focus on articular and fetal growth plate cartilage tissues, the protocols can be applied to other intact animal, plant, and fungal tissues ***(5)***. As we show below, many factors must be taken into account in the choice of experimental parameters, there are no "best settings" that work for all tissues, in all cases.

1.1. Aims

The protocol comprises a series of key methods and associated optimization or correction steps that are necessary to extract and view cell volume data (**Fig. 1**). We describe a microscopy regime, optimizing signal-to-noise ratio and cell viability (**Fig. 2**). As physical interactions between the specimen and light significantly affect the accuracy of the confocal optical probe, we present practical tools to assess tissue-induced attenuation and axial dis-

From: *Methods in Molecular Biology, vol. 122: Confocal Microscopy Methods and Protocols*
Edited by: S. Paddock © Humana Press Inc., Totowa, NJ

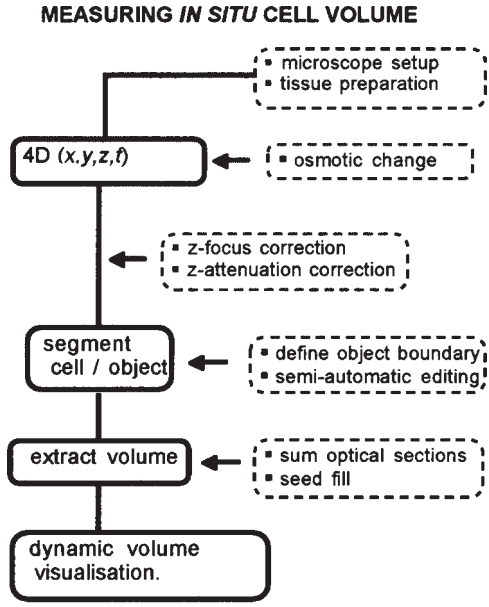

Fig. 1. Schematic summarizing the steps involved in dynamic volume measurements by CLSM.

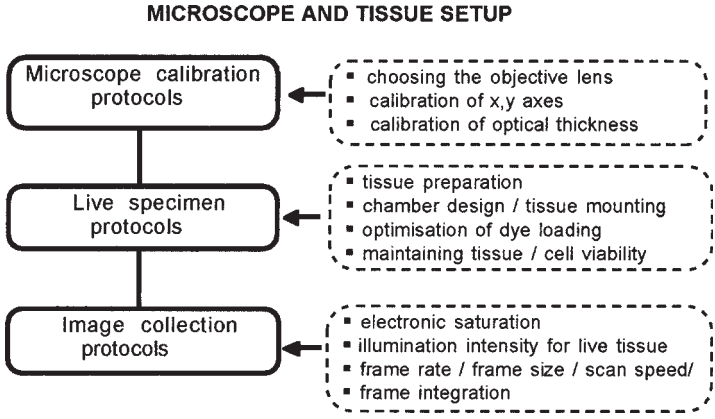

Fig. 2. Schematic summarizing the steps involved in setting up the microscope and optimizing the live specimen conditions.

tortion. Two methods for extracting cell volumes are then given and finally we describe our 4D image visualization methods for the display of dynamic changes in cell volume.

2. Materials

2.1. Biological Material

1. Metacarpal joints of 8-mo-old pigs (used within 4–5 h of slaughter).

2.2. Medium/Buffers

1. Standard: HEPES-buffered DMEM (280 mOsM, pH 7.4)
2. Hypotonic: 1:2 dilution of standard medium (140 mosM, pH 7.4)
3. Hypertonic: standard medium plus 50 m*M* NaCl (380 mosM, pH 7.4)

2.3. Fluorescent Dyes

1. Vital dye: 5-chloromethyl fluorescein diacetate (CMFDA), 2.25 m*M* stock (Molecular Probes)
2. Calibration dye: 50 μ*M* aqueous fluorescein (Sigma Chemicals)

2.4. Preparation of Biological and Calibration Microscopy Specimens

1. Tissue-cover glass adhesive such as: (a) "super glue"; (b) poly-L-lysine; (c) low percentage agarose; (d) medical glue e.g. TissueTAK™; (e) physical method (wire mesh, etc.)
2. Plastic electrical tape to make test chambers
3. Glass slides
4. Cover glass (no 1.5 thickness) (BDH)
5. Tissue fixative: 4% paraformaldehyde in phosphate-buffered saline (PBS).
6. Fluorescein-labeled latex beads (approx the size of cells), e.g., 7 ± 0.3 μm (Polysciences Ltd.)

3. Methods

3.1. Calibration of the Confocal Microscopy Imaging Conditions (Fig. 2)

3.1.1. Choosing the Objective Lens

When measuring cell volume deep within tissue, a major limitation is the working distance of the lens. Data should not be collected from the cut surface, where cells are damaged or undergoing a wound healing response. The finest confocal sectioning requires the maximum possible numerical aperture (NA), (i.e., up to 1.33 for aqueous samples), but a reduced NA of approx 0.8–1.0 may be needed for an acceptable working distance. Although a high NA objective lens provides optimum sectioning near the surface of a preparation, the image becomes less sharp and attenuated when imaging deeper. This occurs often when oil immersion is used and/or with small confocal apertures, further reducing the working distance. The choice of immersion objective lens is not always simple. It is important to use a lens whose prescribed immersion medium matches the refractive index of the bulk of the specimen you will focus

through. Most tissue is hydrated, but the ECM constituents of cartilage (e.g., collagen, fibronectin and proteoglycans) scatter and refract light. Therefore, all objective lenses should be calibrated for measurements (**Subheadings 3.1.** and **8.7.**). For tissue experiments we used a 25x, 0.8 NA Plan Neofluar objective with a variable correction allowing for oil, glycerol or water immersion.

3.1.2. Pixel Size with Different Objective Lenses: Calibration of Image (X,Y) Axes

Since the objective magnification may not be exactly what is inscribed on the lens and the microscope system may have added optical components, the (X,Y) pixel size calibration must be checked.

1. Image a microscope graticule in transmission or reflection mode.
2. Measure the length of the largest number of divisions that will fit the field of view (in pixels). The pixel size (in micrometers) is the total length of the graticule units (in micrometers) divided by the number of pixels.
3. Check this over the image size, zoom and scan speed range you will later use for measurements.

3.1.3. Confocal Pinhole or Iris Setting: Calibrating the Optical Section Thickness

The optical section thickness depends on the out-of-focus fluorescence in the final image (according to the size of the confocal aperture) and the size of the illuminated and detected spots (determined by the NA, wavelength, sample properties, etc). Accurate calculation is difficult for practical cases of high NA, variable confocal aperture and biological specimens. A good compromise is to measure a test sample under the experimental conditions. The axial intensity profile through a simple planar object (much thinner than the axial resolution) gives the plane response function (PRF) from which the section thickness is derived, and *see* **Note 1**.

3.1.4. Axial Response Test Specimen: Reflection Contrast

The PRF is measured from a confocal reflection optical section through a flat mirror (an infinitely thin boundary) deposited on a cover glass using aluminum, gold, or silver as used for SEM specimens (**Fig. 3**).

1. Sputter coat a cleaned no. 1.5 cover glass with the reflective material
2. Mount on a microscope slide with super glue and the mirror surface facing the slide (**Fig. 3A**), and *see* **Note 2**.

3.1.5. Axial Response Test Specimen: Fluorescence

It is difficult to make a planar fluorescent test sample truly subresolution and much easier to derive a PRF from an edge-response sample where fluorescent medium meets an optical boundary (**Fig. 4A**).

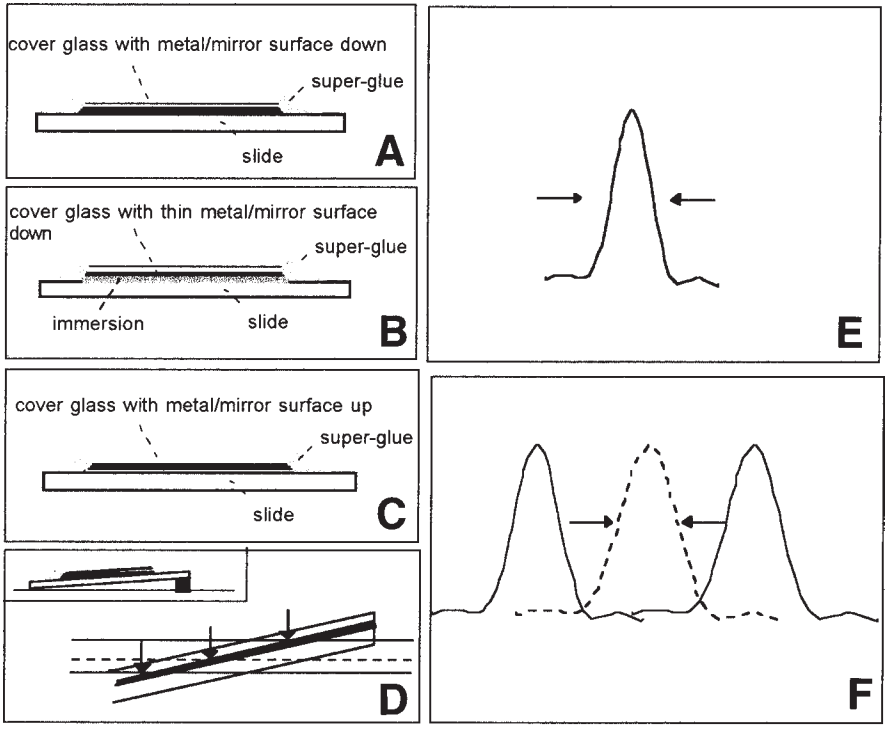

Fig. 3. Measuring the confocal reflection plane response function (PRF). **(A)** Side view of 100% reflecting mirror sputter coated onto cover glass and mounted face down on slide. **(B)** Partially reflecting mirror mounted on slide in immersion medium. **(C)** As in (A) but for objectives corrected for use without cover glass. **(D)** Tilted version of test specimen (inset). Arrows point to intersection of horizontal optical sections with tilted mirror surface (solid band). Calibration sections at two focus positions (solid horizontal lines) and section to measure axial response in centre of field (dotted horizontal line). **(E)** Reflection PRF extracted from vertical (X,Z) section through (A). Arrows indicate the axial width of the peak between the 50% intensity points. **(F)** Reflection PRF plots extracted from corresponding horizontal (X,Y) sections in (D). Arrows indicate width, between 50% intensity points, of central peak corresponding to experimentally determined reflection PRF measurement.

1. Dissolve dye (e.g., fluorescein) in mountant/medium used for biological specimens (50–100 μ*M*).
2. Stick a spacer (~ 200 μm × 25 mm × 25 mm) of foil or electrical adhesive tape onto a slide.
3. Make a shallow chamber by cutting out the center (~10 mm × 10 mm), and *see* **Note 3**.
4. Add 10–20 μL of the fluorescent solution. Avoid overfilling the chamber.

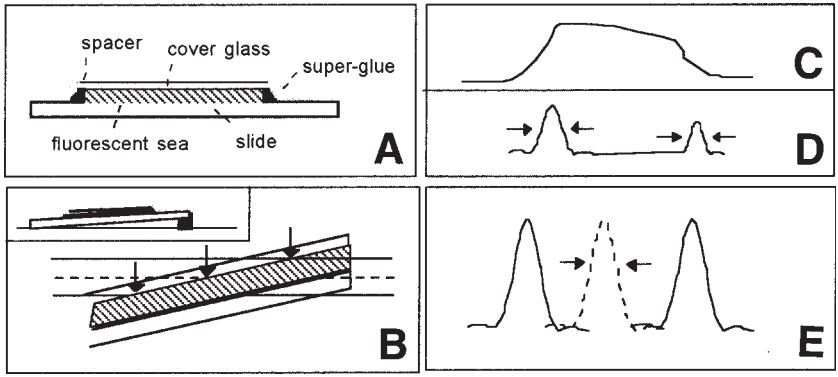

Fig. 4. Measuring the confocal fluorescence plane response function (PRF). **(A)** Fluorescent medium mounted between cover glass andslide. **(B)** Tilted version of test specimen (inset). Arrows point to intersection of horizontal optical sections with cover glass surface and fluorescent medium (hatched band). Calibration sections at two focus positions (solid horizontal lines) and section to measure axial response in centre of field (dotted horizontal line). **(C)** Fluorescence axial response extracted from vertical (X,Z) section through (A). **(D)** Fluorescence PRFs derived by differentiation of the axial response in (C). Arrows indicate the width between 50% intensity points of peaks corresponding to cover glass/medium (left) and medium/slide (right) interfaces. **(E)** Fluorescence PRF plots extracted from corresponding horizontal (X,Y) sections in (C). Arrows indicate width, between 50% intensity points, of central peak corresponding to experimentally determined fluorescence PRF measurement.

5. Slowly lower a cover glass onto the chamber, avoiding air bubbles.
6. Seal with super glue.

3.1.6. Collecting the Axial Response Using the Motorized Focus

The confocal microscope focus is usually controlled by a motor in steps of approx 50–100 nm. The accuracy (of the mechanical stage movement), when transmitted through the microscope to the specimen, is always worse than this (even with temperature control) but estimates of the axial performance can be made with this method (**Figs. 3A** and **4A**).

1. Set up the required microscopy conditions, ensuring the system is correctly aligned.
2. Mount the reflection or fluorescence test specimen securely on the microscope stage.
3. Collect a vertical (X,Z) section or a 3D (X,Y,Z) z-series across the boundary. For low NA lenses or non-ideal conditions several micrometers on each side should be scanned initially to capture the full axial response, and *see* **Note 4**.
4. Measure an intensity z-profile across the boundary (averaged in X/Y to reduce noise) (**Figs. 3E** and **4C**).

3.1.7. Extracting the PRF from the Fluorescence Axial Step-Response

The PRF is approximated by the first differential (gradient) of the fluorescence Z step-response (**Fig. 4C,D**).

1. Export the boundary profile into your spreadsheet package.
2. Generate the gradient plot (e.g., the difference between neighbouring points).

3.1.8. Collecting the Axial-Response with a Single (X,Y) Section

When the Z-response must be assessed repeatedly, or more accurately than the focus steps allow, (X,Y) scanning is used. By slightly tilting the test specimen the boundary plane passes through the focus across the field of view (**Figs. 3D** and **4B**). An (X,Y) section through the boundary gives the z-response, and *see* **Notes 5** and **6**.

1. Set up the required imaging conditions, ensuring the system is correctly aligned.
2. Attach a spacer (~1 mm) at one end of the test slide.
3. Calibration using the known tilt : mm (Z) per pixel (X,Y) = tilt/(X,Y) pixel size in mm.
4. Calibration using two (X,Y) sections with a focus difference (df): mm (Z) per pixel (X,Y) = df (μm)/distance between boundary centers (**Figs. 3D,F** and **4B,E**).
5. Store the calibration as the image x-increment and use to convert later measurements.
6. Collect an (X,Y) section with the boundary in the centre of the field. Measure an intensity X-profile across the boundary (averaged in y to reduce noise) (**Figs. 3D,F** and **4B,E**).

3.1.9. Extracting the Optical Section Thickness from the PRF Data

The complete optical section is the distance between the first minima on either side of the PRF central peak. A better practical measure is the width between the 50% intensity points (**Figs 3E,F** and **4D,E**).

3.1.10. Setting the Optimum Confocal Aperture Iris Setting

Three things happen to a confocal image as the aperture closes: First, out of focus blur steadily reduces, giving more contrast. Second, near the optimum contrast (under ideal conditions) resolution should increase to a final value, and will not then change if the iris is closed further. The third effect is a pronounced loss of intensity. Sectioning and resolution are balanced against the signal-to-noise ratio and must be determined empirically. About 15–20 sections per cell (~10 μm) are needed to measure cell volumes in cartilage tissue and focus steps should ideally be half the section thickness, (e.g., 0.5 μm steps and 1.0 μm sections). The confocal aperture is key as it influences (1) section thickness, (2) signal-to-noise, (3) resolution/contrast, and (4) depth attenuation. Test specimens are a starting point for optimizing the biological experiment.

3.2. Cartilage Tissue Preparation

1. Remove 20 mm × 10 mm × 3 mm cartilage explants from the ridge of porcine meta-carpal joints, and *see* **Note 7**.
2. Cut approx 1 mm slices longitudinally and suspend in standard HEPES-buffered DMEM.

3.3. Vital Dye Loading

1. Incubate the tissue in standard medium containing 4.5 μ*M* CMFDA at 37°C for 15 min, and *see* **Note 8**.
2. Wash in fresh medium
3. Leave for a further 10 min to ensure all of the dye-ester is cleaved by intracellular enzymes.

3.4. Mounting the Tissue in the Observation Chamber

1. Place the tissue in a heated chamber (37°C) with perfusion (2 mL/min).
2. Mount the chamber on the microscope (we used a Bio-Rad MRC 600, with a Nikon Diaphot)
3. For perfusion, use a chamber inlet supplying fresh medium close to the cover glass and aspirate the spent medium from the top (*see* **refs. *7,8*** for details of some available chambers).

3.5. Optimizing Image Collection

3.5.1. Fluorescence Image Statistics: Avoiding Detection Saturation

For quantitative images, all signal must be accomodated within the detection limits (e.g., 8 bits, 0–255).

1. Focus into the cover glass of the chamber and scan single (X,Y) planes, with no averaging.
2. Plot a histogram of the pixel intensity distribution after each scan.
3. Adjust the black level so that all intensities are recorded above a gray-level of 15.
4. Adjust the gain and/or laser power so the maximum histogram intensity is below 240.
5. Alternatively, use a range check display LUT indicating these limits, e.g., green (0–15), gray scale (16–239) and red (240–255). Ensure no pixels in a single (nonaveraged scan) are colored.

3.5.2. Image Collection Conditions

1. Ideally, control the laser power (directly or by neutral density [ND] filters) at the specimen using a power meter (typically 20–100 μW for physiological specimens).
2. An iterative process should be used to establish the instrument settings: Our aim is to collect 4D images where neither the tissue nor fluorophore are disrupted. Use PI as a viability marker and mean intensity/variance of a homogenous region to assess signal-to-noise ratio.

3. Set the frame rate by independently adjusting frame size and scan speed/pixel dwell time.
4. CLSM offers many different time-lapse modes. Select either 3D (X,Y,Z) "Z-series" imaging and auto/manually repeat for different time points or 4D (X,Y,Z,T) imaging (if your system supports this).
5. Set the frame averaging to balance noise reduction (s/n increases by the square root of the no. of frames), against photobleaching and lower temporal resolution, and *see* **Notes 9** and **10**.

3.6. Experimental Regime: Chondrocyte Volume Regulation In Situ

The following protocol is for collecting 4D images through chondrocytes *in situ* under anisotonic conditions ***(4)***. From osmotic rest, we apply a short swelling stimulus followed by hypertonic shrinking and then follow the regulatory volume increase.

1. Mount the cartilage as described previously.
2. Set up the microscope for fluorescence, ensuring the gain and black level are correctly set for the specimen region you will image (*see* optimizing the imaging conditions above).
3. Perfuse with standard DMEM (280 mos*M*) and collect the initial 3D image of the 4D series.
4. Replace the medium with a hypotonic solution: the swelling stimulus (140 mos*M*)
5. Collect a series of 3D images at 5-min time intervals for 10 minutes.
6. Replace the medium with a hypertonic solution: the shrinking stimulus (380 mOs*M*).
7. Collect a series of 3D images at 2-min intervals for 15 min.
8. To ensure the preparation is physiologically sound, collect a final 3D image 30 min later.
9. The result is a 4D image, composed of a series of 10–12 3D images.

3.7. How Does the Specimen Affect the Imaging? Calibrating the Sample Induced Errors

*3.7.1. Calibration of Axial Attenuation (**Fig. 5**)*

It is important to record exactly how the live data was collected, to replicate the conditions, so that the calibration can be meaningfully applied to 4D data. Features that effect axial attenuation include: (1) objective lens (plus correction collar setting if available); (2) pinhole/iris setting; (3) excitation/emission spectra; and (4) explant tissue or segments.

It is best to use the same piece of tissue for calibration (e.g., at the end of each experiment), but accurate attenuation assessment requires penetration of the cartilage with fluorescein, which can take 48 h. The explant site must therefore be accurately logged to locate an equivalent region for calibration.

1. Fix the tissue in 4% paraformaldehyde in PBS (24 h for cartilage, less for other tissues).

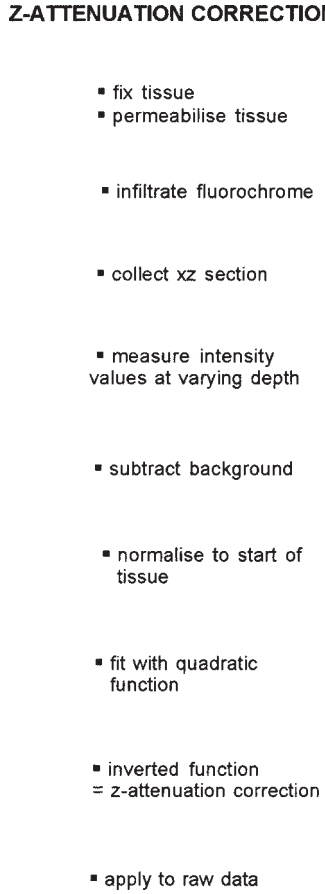

Fig. 5. Schematic summarizing the steps involved in axial attenuation correction.

2. Incubate in aqueous 50 μ*M* fluorescein for 48 h to ensure dye penetration, and *see* **Note 11**.
3. Mount the tissue in the chamber surrounded by fresh fluorescein solution (**Fig. 6A**).
4. Set up the microscope ensuring the gain and black level are correctly set (*see* **Subheading 3.5.1.**).
5. Collect a 2D (X,Z) section or 3D (X,Y,Z) image of the tissue over the experiment Z-range.
6. Measure the image black level as the average intensity collected with no laser illumination.
7. Plot a vertical intensity profile (averaged across a homogenous region in the X dimension) through the vertical section and export this to your spread sheet package.
8. Subtract the average black level from all the values in the intensity profile.

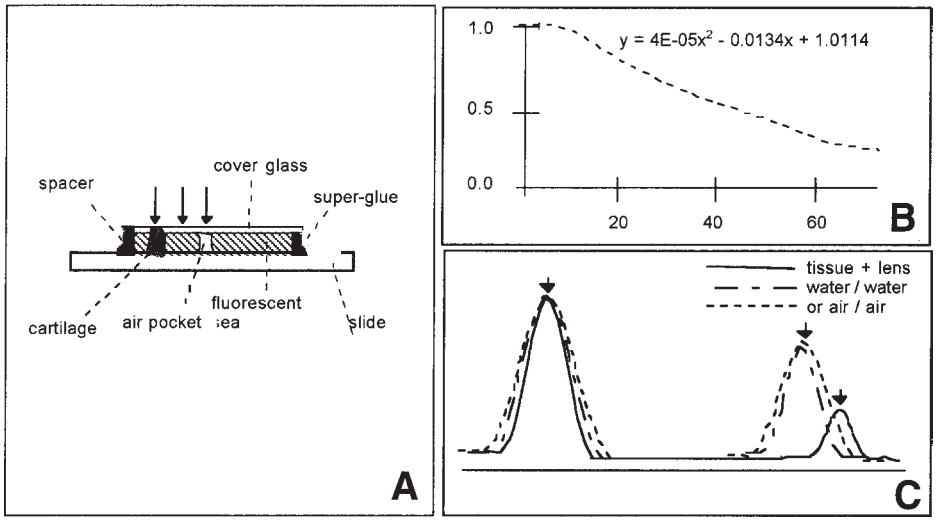

Fig. 6. Calibrating the specimen-induced attenuation and axial focus distortion. **(A)** Fluorescence test specimen (as **Fig. 4**) with the addition of biological material and reference (fluorescence sea or air pocket). **(B)** Measured axial fluorescence attenuation response through cartilage impregnated with fluorescein. Intensities are normalised to value at top of biological material. Quadratic parameters fitted in Microsoft Excel are shown. **(C)** Axial reflection PRF plots through the biological material (**solid line**) and reference regions (**dotted lines**). Arrows point to the peaks corresponding to cover glass/medium (**left**) and medium/slide (**right**) interfaces.

9. Normalize the intensities to the first point in the tissue, this then gives the relative axial intensity change owing to the combined optical and tissue-dependent attenuation (**Fig. 6B**).
10. Parameterise the normalized data by fitting a trend line (e.g., quadratic: $Y = aX^2+bX+c$) (**Fig. 6B**).
11. Subtract the black level from all images and divide by the attenuation for each Z-position (**Fig. 7**).

3.7.2. Calibration of Z-Focus Distortion

Refractive and scattering boundaries in biological specimens result in significant aberrations in confocal microscopy. There is an axial focus shift and attenuation when the spherical wavefront coming from the objective, or specimen, passes between immersion and mountant with unmatched refractive indices. Specimens with horizontal planar or other continuous refractive index boundaries may also show this effect. Distances measured in the sample must be corrected by a factor that approximates to (sample refractive index)/(immersion refractive index). For some combinations of immersion and

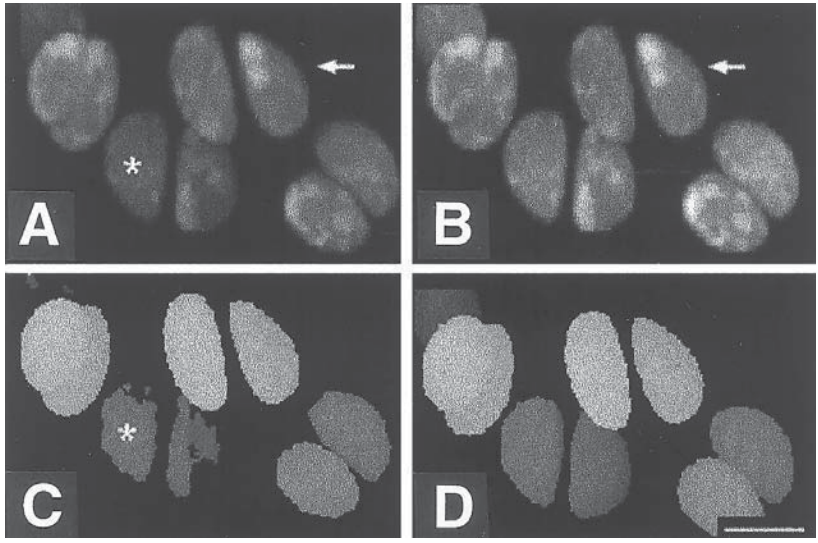

Fig. 7. Correction of sample-induced axial attenuation for in situ chondrocytes in cartilage explant. **(A)** Maximum projection of a single uncorrected 3D time point. Asterisk shows a cell with a lower apparent fluorescence intensity and deeper into the tissue volume than the neighboring cells. Arrow shows brighter cell nearer the surface. **(B)** As in (A) after correction of axial attenuation. Cell nearer tissue surface (**arrow**) and deeper cell now have similar fluorescence intensity. **(C)** Height coded projection of data in (A). Asterisk shows cell deeper into the tissue incorrectly visualized owing to the axial attenuation. **(D)** As in (C) after correction of axial attenuation.

medium or sample the factor may be up to 5% different from this ratio in confocal microscopy or the refractive indices may be unknown. Under these circumstances a value is determined empirically (**Fig. 8**).

1. Prepare the fluorescence test specimen chamber as described previously but thick enough to just accommodate a 100 µm thick piece of tissue (just a few microns of medium above and below).
2. Place a representative specimen into one half of the chamber. Fill with medium and seal.
3. Collect a reflection PRF profile (described above) through the cover glass, tissue, and into the slide (below the tissue). Use the objective you normally use for physiological experiments (**Fig. 6C**).
4. Repeat **step 3** with a cover glass corrected water immersion lens through the clear part of the chamber, and *see* **Note 12**.
5. Measure the distance between the two medium/glass boundaries for the tissue and reference.
6. Measure the width of the optical sectioning as indicated by the PRF above the specimen and below, and *see* **Note 13**.

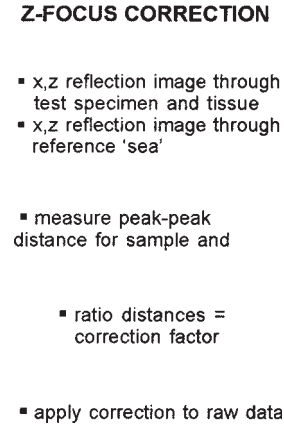

Fig. 8. Schematic summarizing the steps involved in axial focus correction.

7. The ratio of the distances in **step 5** gives the Z-focus error (a factor to apply to all Z-distances)
8. The difference between the estimates in **step 6** gives an estimate of sectioning distortion.

3.7.3. Confocality, Optical Section Thickness, and Object Dimensions

Our measurements of volume require the optical section thickness to be much smaller than the size of the object. The confocal microscopy image can be described as each fluorescing point in the object, replaced, or imaged as a volume element with the dimensions of the microscope resolution, i.e., a few hundred nm in (X,Y), (depending on the NA and confocal aperture), and the optical section thickness in Z. Because the section thickness is always greater than the (X,Y) resolution by at least a factor of three, the major error is an inflation of the Z-dimension of objects by at least one optical section thickness. The precise effect at the boundary of an object depends on the radius of curvature of the edge compared with the microscope resolution ***(9)***. For low NA lenses, or with large confocal apertures this can lead to overestimation of volumes. The only simple solution is to use a higher NA lens and/or smaller aperture. When this is not possible, i.e., for depths of many hundreds of microns into tissue, two more involved options may have to be considered. The first is to use computational deblurring (e.g., deconvolution) software to partially restore the correct dimensions of the object. This subject is fully discussed elsewhere ***(10)***. The second, more pragmatic approach, is to measure a test object of the same shape and dimensions as your cells using the imaging protocol in question. A rough indication of the size inflation can then be calibrated by ratioing the measured size with an independent estimate by, e.g., light scat-

tering, Coulter Counter etc. A representative but thinner preparation could also be used for this calibration and imaged with a high NA objective.

3.8. Segmentation: Objective Determination of the Cell Boundary

To accurately measure the volume of labelled cells (positive or negative), an objective estimate of the cell boundary position must be made. The threshold used to segment an object profoundly affects the apparent volume ***(4,5)***. The position of this boundary for positive labelling is somewhere between the maximum intensity (definitely within the cell) and the minimum intensity (definitely within the extracellular matrix).

3.8.1. Defining the Boundary Threshold Rule Using Fluorescent Beads

1. Find the modal value of fluorescent bead diameters (~ 7 µm) by Coulter Counter (**Fig. 9A**).
2. Obtain 3D images of the beads adhered to a cover glass coated with 0.1% (w/vol) poly-L-lysine.
3. Select a central section through the beads.
4. Measure an average intensity within a bead and for a background region.
5. Obtain a series of intensity thresholds as a percentage of the maximum intensity above background, i.e.:

$$[X \cdot (I_{\text{cell}} - I_{\text{background}})] + I_{\text{background}} \qquad \text{e.g., for } X = 0.3 \text{ to } 0.7$$

6. Generate a maximum Z-projection (see 3D visualization below) of the image data.
7. Binarise the projected image by setting all pixel values below X to 0 and all values above X to 255.
8. Obtain estimates of bead diameter (area of cross-section/3.1416). Plot a histogram (**Fig. 9**).
9. Compare the modal values from the confocal microscopy and Coulter Counter distributions.

Diameters of 7 µm beads by Coulter Counter and confocal microscopy (50% threshold) correlate well, and *see* **Note 14**.

3.8.2. Segmenting the Chondrocyte Data

1. Segment the CMFDA-stained cells from the cartilage images (as for the bead calibration previously described). Determine background and cell intensities on a cell by cell basis, avoiding errors from uneven staining.
2. Obtain confidence limits for the boundary thresholds at 50% ± 1 SD of the cell intensity. For example, for a 50% threshold

(i) $$0.5 \cdot (I_{\text{cell}} - I_{\text{background}}) + I_{\text{background}} = (I_{\text{cell}} + I_{\text{background}})/2$$

(ii) $$(I_{\text{cell}} + I_{\text{background}} + I_{\text{std}})/2$$

(iii) $$(I_{\text{cell}} + I_{\text{background}} - I_{\text{std}})/2$$

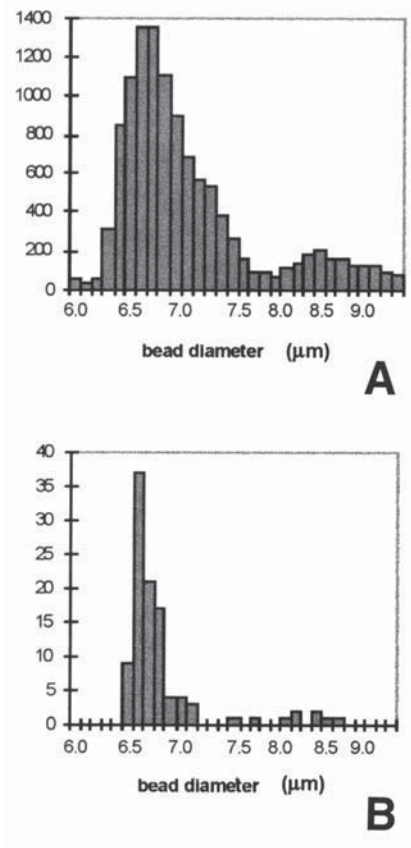

Fig. 9. Diameters of 7 µm fluorescent beads determined by Coulter Counter and confocal microscopy. Histograms of bead diameter distributions. (A) Coulter Counter (mode = 6.64mm). (B) Confocal fluorescence microscopy (mode = 6.6 mm).

3.9. Two Methods for Extracting Cell Volume

You can now use the segmentation thresholds to measure volumes in 3D time points or 4D image series.

3.9.1. Summing Cross-section Areas

For each cell in the volume (**Fig. 10A**):

1. Analyze the (X,Y) optical section through the cell.
2. Determine the cross-sectional area above the threshold intensity in pixels or micrometers (**Fig. 10B**)
3. Determine the cross-sectional area for the two confidence limits.
4. Sum the areas for all sections through the cell.

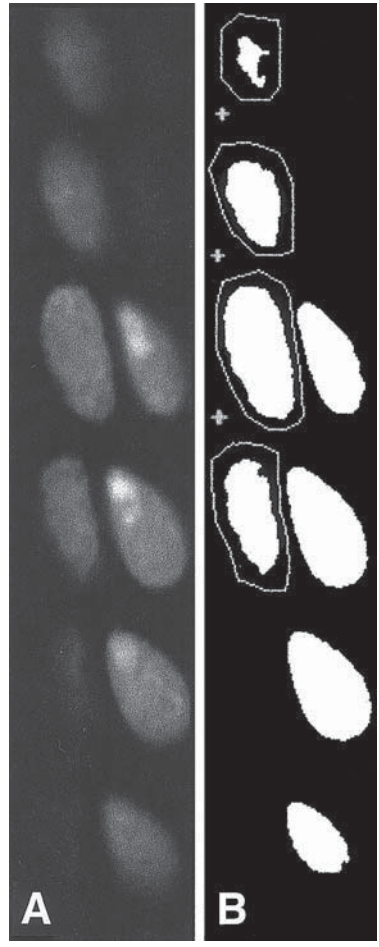

Fig. 10. Measurement of *in situ* chondrocyte volumes by summing optical sections. Six optical sections through two cells fluorescently stained with CMFDA. **(A)** Raw image data. **(B)** Data in (A) after binarisation based on 50% intensity threshold between background and mean cell intensity.

5. Convert the sum into volumes for each cell (and confidence limits) by multiplying a pixel area by the product of X, Y, and Z pixel spacings) or multiplying an area in mm by the corrected Z spacing, and *see* **Note 15**.

3.9.2. 3D Segmentation

Some software packages can automatically segment 3D objects without processing each section separately ***(11)***. These use a threshold or other boundary-condition algorithm, searching for image voxels that are connected to each

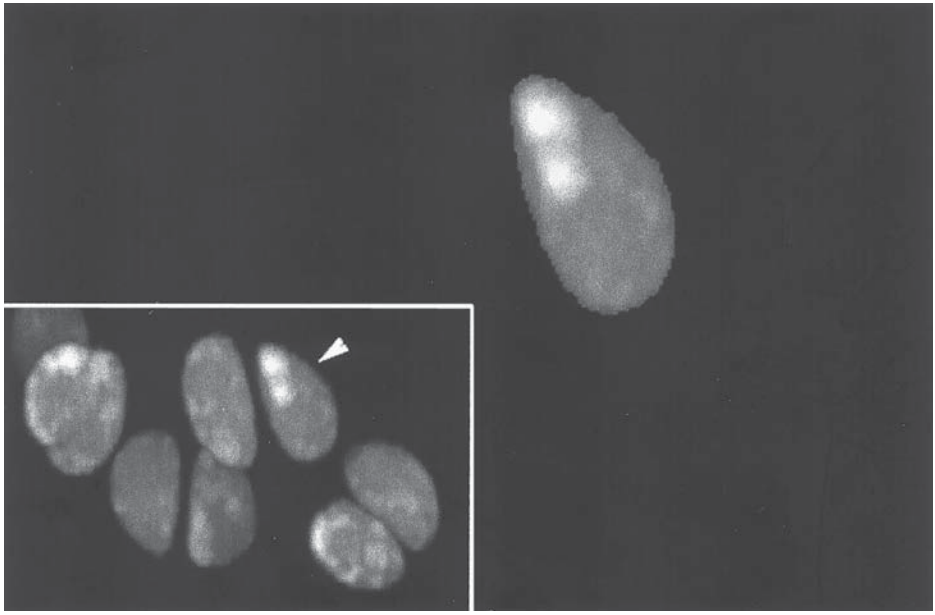

Fig. 11. Measurement of *in situ* chondrocyte volumes by seed filling. Maximum projections of 3D confocal fluorescence images. A single cell (**arrow**) extracted from one time point (**inset**) by voxel seed filling.

other. Different versions allow for various degrees of connectivity between adjacent voxels to include in the object. The seed fill algorithm starts inside the object at a seed position determined manually or (semi-)automatically, filling out the object to the boundary and reporting the volume (**Fig. 11**).

3.10. Visualizing Volume Data

The amount of data collected in a typical 4D confocal microscopy image (often 10s or 100s of Mb per experiment) results in many logistical problems for analysis, data manipulation and visualization. It is important to consider multidimensional visualization as selective data reduction. A 3D data set, or sub volume from a 4D series, must be reduced to a 2D view for display on a monitor, printout, slide etc. Some display systems, such as computer or video screens, allow sequences of 2D views to be presented and most can use 3D effects to aid the interpretation of the presented data. Visualization requires the projection of 3D/4D data onto one or more 2D planes, the data intensities being rendered into display 'views' in such a way as to retain some important features. The result is then presented to an audience, using additional effects or processes to partially restore the "3D/4D nature" of the original data. We strive

to make the most efficient use of the available display resources using the simplest projections and rendering to maximize the audiences ability to understand what they see with the minimum of misinterpretation ***(12)***.

A typical confocal data visualization session would normally progress from simple section animations to data projections of increasing sophistication including stereo and other display techniques.

3.10.1. Displaying 2D Sections Through the 4D Image Data

1. Ensure the images are correctly scaled to fill the range of the display device (0–255 gray levels, for 8 bit data). Measure the minimum and maximum intensities (of the entire image) and then either rescale all the values or simply using the intensity limits to control the display look-up-table (LUT), and *see* **Note 16**.
2. Ensure the dimensions (X, Y, and Z pixel sizes in μm) are correctly represented in the file format and/or the display software, otherwise images displayed outside of the microscope software or computer system may not retain the correct proportions. In particular ensure that the axis calibrations have had any necessary corrections.
3. Use the section display/animation tools to show a sequence of views as if focussing along each of the three main axes of the data. Some display packages may not be able to do this sort of animation rapidly for anything other than standard Z series of (X,Y) sections, Y series of (X,Z) sections, etc. Many will allow general sections at any angles to be precalculated for later animation, and *see* **Note 17**.
4. Use the section animation tool to view a time series at a single Z-focus position (if your software will allow this). If this capability is not available in your software, you should be able to rearrange the data so that , e.g., it is organised as a series of files containing timelapsed (X,Y), (X,Z), etc. sections, each file corresponding to a particular focus level, rather than each time point in a separate file.

3.10.2. Simple 3D Projections

Only a single value is required for each pixel in a 2D view. During a 3D projection, voxels are traced along lines cast through the volume, in the direction of view, and processed to yield a single value at each view pixel (e.g., **Figs. 7** and **11**). Processing rules'for simple ray cast projections include the maximum brightness (e.g., for surface reflections, sparse fluorescence staining, etc.) or the mean value (a good unbiassed method for an initial view). It may be necessary after projection to rescale the view for optimum contrast.

1. Use the simple projection functions in your visualisation package to make a single 2D view of each 3D time point of the 4D data. Store these views in a single file and then animate the time series, and *see* **Note 18**.
2. Now use the projection tool to make several 2D views of just one 3D time point but from a range of viewing directions (e.g., a series with tilt and/or rotation steps).

3.10.3. Voxel Surface Visualization: Height or Depth Views

To help restore depth in the views, some algorithms render the first or front voxel nearest the viewer. This gives a surface effect (but no connection is necessarily assumed between adjacent voxels). These surface voxels are represented either by their original intensity or by a brightness coresponding to their depth, height, or Z-coordinate in the data volume. Surface projection modes have the effect of hiding the data voxels behind and/or within the structure, conveying a sense of solid character to the view. Always use the section animation tools previously described to review the entire data volume before making solid reconstructions.

1. Recall the objective estimates of boundary thresholds for the 4D images of CMFDA-stained cells.
2. Use these values as the surface threshold in a surface or height projection, and *see* **Note 19**.
3. Use the visualization tools to make a surface view at each 3D time point. Animate these to see the changing morphology of the cells over time (**Fig. 12**).
4. The display colour now represents the height of a voxel, looking into the volume. Use a colour display LUT to highlight cells near the front of the volume, middle or further back, etc. Find a pre-set LUT like the standard geographical colours in an atlas (blue/black for valleys, red/grey for peaks etc.) to show topographical features. Alternatively, use a single narrow color band (e.g., a 10 level-wide red band) and move it over the grey scale to contor different topographical features of the surface view.

3.10.4. More Advanced Visualization Tools

Alpha blending ***(12)*** is a tool very similar to the projection techniques described above that is available in some visualisation packages. Ray casting is used and the data is traversed either away from or towards the viewer. Each pixel of the 2D view is determined by first multiplying voxels along the cast ray by an opacity or alpha value that simulates masking of voxels behind it in the volume. High opacity voxels will appear as solid features near the front. Bright voxels towards the back of the data volume will tend to show through more transparent data near the front. Alpha blending requires careful control of the alpha function used to map data values to opacity/transparency attributes which confer an artificial material character to the raw data. The alpha function must be inspected with the rendered views, otherwise you cannot unambiguously separate, e.g., dimmer voxels from bright regions masked by overlying opaque structures.

We used an alternative approach to visualize chondrocyte volume data by a combination of average projection (conserving original fluorescence intensity values) and surface visualization (show the cells at the front of the volume

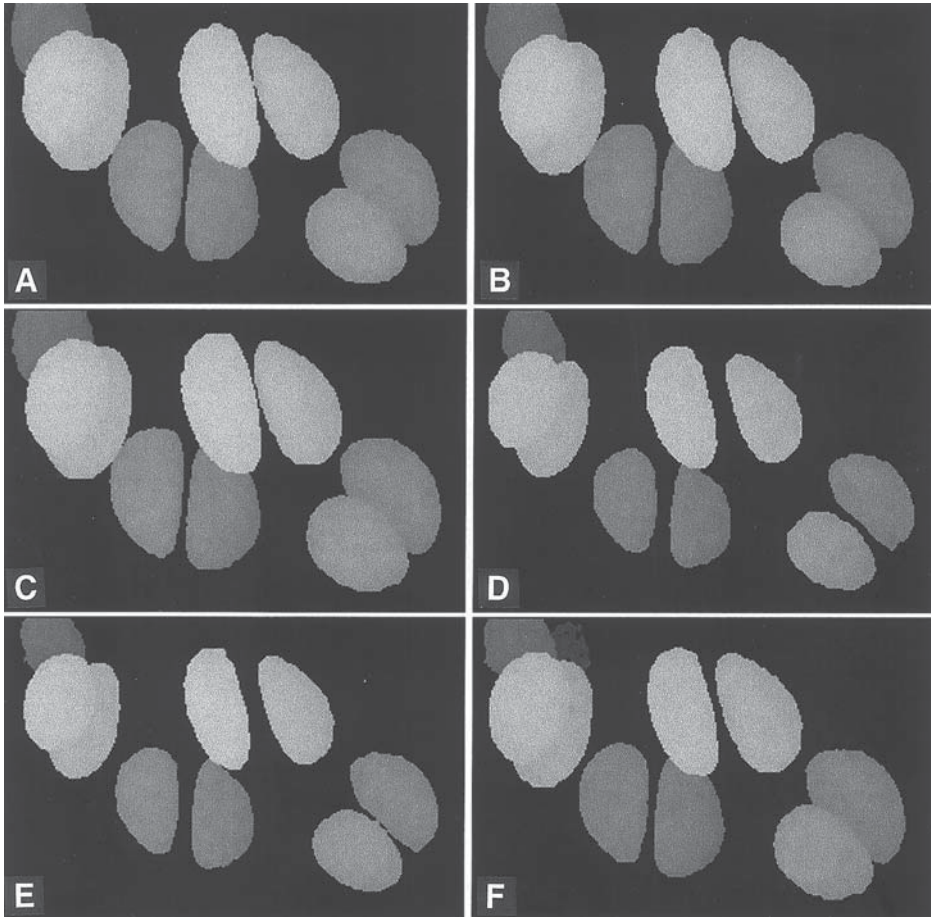

Fig. 12. 4D visualization of in situ chondrocytes undergoing volume regulation. Six time points **(A–F)** during a one-hour physiological experiment manipulating osmotic load. A 3D confocal fluorescence image collected at each time point is visualized as a height coded projection. (A) 0 min (280 mosM). (B,C) 5–15 min (140 mosM hypotonic swelling stimulus). (D) 20 min (380 mosM hypertonic shrinking stimulus). (E,F) 25–60 min (380 mosM). Cells respond by regulatory volume increase.

occluding the cells behind. We have also devised a second type of 4D reconstruction that uses color to represent relative changes in cell volume, hence contrasting individual and population volume responses. This process is not fully implemented in the standard commercial CLSM packages, but it is possible with many systems to produce output as presented below. We describe the process, step by step below, using a combination of standard components, with a details of the new techniques we have added.

1. Use the boundary thresholds defined above to generate height coded views of each time point.
2. On a pixel-by-pixel basis, use the height image to define a reference surface about which to apply a limited or 'local' average intensity projection (i.e. ,from a few voxels in front to a few voxels behind the surface). In this way a layer around the outer region of the cell is rendered, showing the mean fluorescence intensity. By increasing the distance projected, the cell becomes more transparent, and *see* **Note 20**.
3. Animate these reconstructions (in rotation, tilt, etc., or over time depending on how you have made them) to see the staining pattern of the cells and their arrangement in the tissue.

3.10.5. Visualizing Cell Volume Using a Depth Sensitive Color Display

1. Seed fill each cell in turn (as described above) and render the voxels of each cell, using the two pass method described above, into the view.
2. Maintain a height (Z-coordinate) view of the result as it builds up.
3. Convert the volume of each cell to a relative volume by normalising to the first time point.
4. Generate a height (Z-coordinate) view of each cell.
5. As each cell is rendered into the view (in **ref. *1***), the height view (in **ref. *3***) is compared with that of the final result and only the front-most voxels are rendered onto the display. In this way, cells at the front of the volume obscure cells behind.
6. Generate the rendered view as a 24-bit color image, each voxel contributing an intensity corresponding to its brightness in the projection proportioned between the three channels according to an RGB colour ratio. Obtain this ratio by passing the relative cell volume through a topographic colour LUT to provide the necessary red, green, and blue components.
7. Now observe a single visualized 3D time point to see the relative volume of each cell in the volume.
8. Animate a rotation series of one time-point to see the detailed 3D disposition of the cells and any correlation with their relative volume.
9. Animate a series of volume-coded reconstructions made at each time point to see the dynamic volume changes as transitions through different colors. You should be able to see subtle volume changes that are not apparent by the small changes in the linear dimensions observed in a monochrome view.
10. Finally, make a montage of each visualized time-point together with a graphical plot of the relative volumes during the physiological experiment (**Fig. 13**).

4. Notes

1. The PRF is often confused with the point spread function (PSF) obtained by serially sectioning sub resolution fluorescent beads. Profiles through the PSF give the Z- and X/Y- resolution, but the total intensity in each plane gives the axial PRF. Brownian motion of low intensity beads makes these measurements unreliable in aqueous samples.

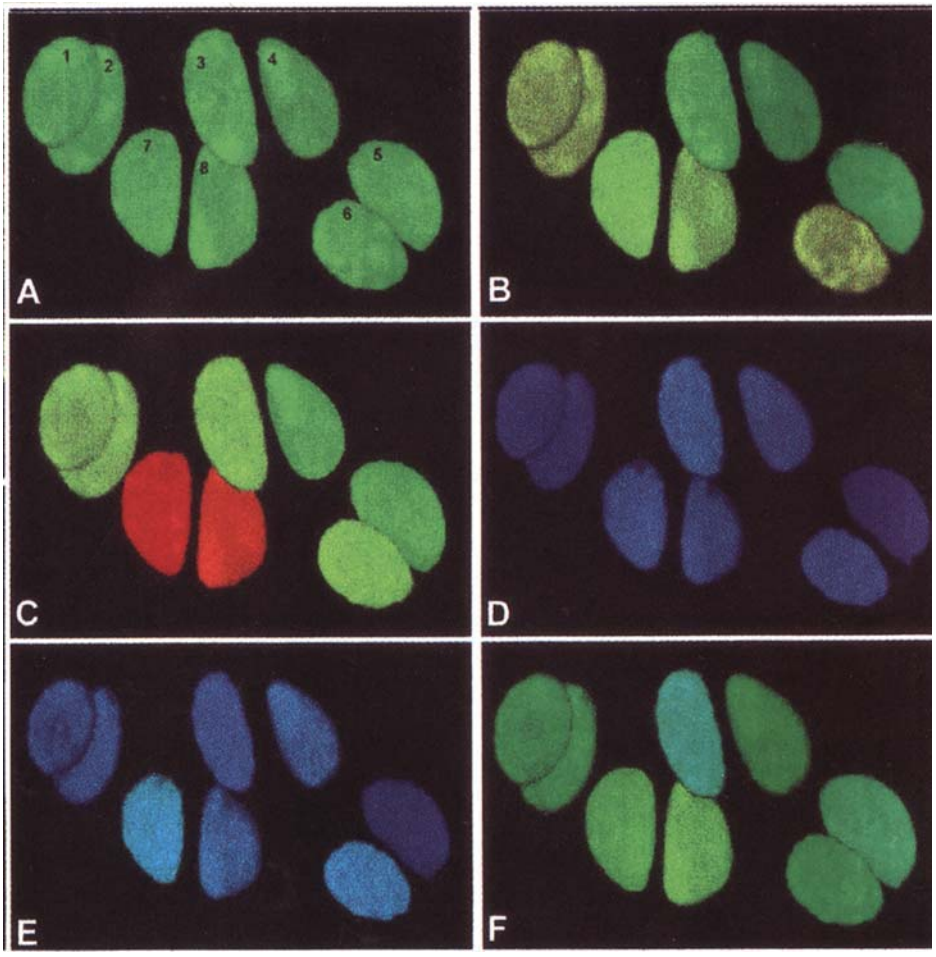

Fig. 13. 4D visualization of *in situ* chondrocytes by colour coded relative volume changes. Six time points **(A–F)** (as in **Fig. 12**). (A) Cells at initial time point have relative volume = 1 (green, shown here in mid gray). (B,C) Cells swell to a relative volume > 1 (yellow-red, shown here in light gray) asynchronously and to different extents (0.89–1.1). (D) Cells shrink to a relative volume < 1 (blue, shown here in dark gray) coordinately (to 0.56–0.66). (E,F) Cells slowly increase their relative volume (cyan–green) achieving a mean recovery of 0.92 (0.82–0.92). (*See* Color Plate I.)

2. If the metal layer passes light through to the slide, this may reflect back causing interference fringes. Thin metal layers should be mounted towards the slide in immersion oil sealed with super glue, or solid mountant with the refractive index of glass (**Fig. 3B**). For an NCG (no cover glass) lens the mirror is mounted toward the objective lens (**Fig. 3C**).

3. See dye data sheets for solubilities (e.g., DMSO may be needed for some dyes in water). Rhodamine 6-G, Ex 514 nm, Em > 590 nm, (Eastman Kodak) dissolves in water, glycerol, and oil.
4. With immersion objectives, focus so that force applied to the specimen is towards the stage (i.e., stage and lens approaching on upright microscopes or moving apart on inverted). This limits axial errors if the sample is not compressible or extendable. Sample distances must be adjusted by the ratio of medium/immersion refractive indices.
5. Use the sharpness of the peak in this reflection Z-response to fine tune the alignment of a confocal microscope.
6. The second method is more accurate if the stage is not perfectly orthogonal to the optical axis.
7. The tissue is placed into a physiological medium that must maintain the cells at the desired osmolarity. Removing explant tissue often causes swelling, so sucrose and sodium chloride are used to increase medium osmolarity. HEPES eliminates the need to supply CO_2 during the experiment, and buffers pH so that the tissue is not exposed to acid load.
8. Other dyes (e.g., BCECF*, calcein) may be used to measure volume but during cell swelling and recovery dye leaks and/or is pumped from the cell. CMFDA is retained better as it covalently binds to intracellular thiols. To avoid disruption of cell function at high dye concentrations, ascertain the upper limit of loading consistent with normal physiology before optimizing the microscopy conditions. This requires objective markers of function in loaded and unloaded cells, for example; membrane potential or integrity [e.g., propidium iodide or PI ***(6)***], cytoplasmic streaming, metabolic activity, growth rate, etc.). The ECM excludes large molecules, has highly charged proteoglycans and cells may leak enzymes that cleave dye-esters. Loading may be enhanced by adding enzyme (e.g., protease) inhibitors.
9. It is not always clear whether the best signal-to-noise vs cell viability regime is single slow scans or faster scans with integration, as this usually depends on the fluorochrome relaxation time and is heavily influenced by the environment.
10. For many of our 4D physiological cartilage experiments on a MRC 600, we used a 25× 0.8 NA objective, image size = 768 pixels × 180 lines × 40 frames (0.21 × 0.21 × 1.0 µm voxels), scanning at three frames/s with two-frame integration. This 3D image was repeated every 2–5 min for one hour. Laser excitation (at the sample) was ~ 20 mW, intracellular dye (CMFDA) concentration ~ 5 m*M* with a confocal aperture ~2 mm.
11. Fluorescein was chosen, because its fluorescence is similar to CMFDA but, unlike CMFDA, it stains fixed cells. Strictly, the attenuation profile starts at the cover glass/medium boundary and should include the medium above the specimen. If you normalise to the top of the specimen itself you should collect the experimental data with the tissue at the same distance from the cover glass. For a water immersion or low NA objective the error is small.

*2',7'–Bis (2–carboxyethyl–5,6–carboxyfluorescein.

12. If you do not have a CC water immersion lens, you will have to make this reference section through an air pocket trapped in the medium when you make the specimen and image with an air lens (**Fig. 6C**).
13. The integrated intensity of the PRF responses above and below the specimen should correspond to the attenuation curve determined earlier. Any differences may reflect small changes due to fixation.
14. Take care when using beads to calibrate axial dimensions, including volumes, for CLSM. Some beads have a significantly higher refractive index than water (often over 1.6). These act like lenses, focussing the light with the effect of lengthening apparent axial dimensions measured in the bead and asymmetric axial blurring.
15. In some software packages, semi- or fully-automatic procedures may be available to segment these cross sectional areas. It may, alternatively, be necessary to work with (X,Z) sections if the object is particularly flattened in the axial direction (to avoid significant errors at the top and bottom of the structure).
16. For 8-bit images, software packages allow the image values to be represented on the screen in several ways. The simplest is to use a grey scale (equal amounts of red, green, and blue for each value) directly related to the voxel value. Data values are mapped through the display LUT and the output red, green, and blue colors are displayed on the screen. To enhance areas of similar intensity a nonlinear color LUT is used to map brightness to particular hues (combinations of red, green, and blue). Such techniques are widely used to display subtle changes in ion concentrations stored as the emission ratio of dual wavelength ion-sensitive dyes. This way of coloring 8-bit data is usually called ‘ndexed color. When multiple-channel images (e.g., from several confocal detectors) or the output from a color camera are displayed, the data usually exist as three 8-bit values, each representing a separate level of red, green, or blue. The final color displayed is not determined by mapping values through a LUT but by altering the actual value stored in each color plane. This is normally called 24-bit or true color. Because of the increased amount of data, and the need to change stored values to change the display colors, 24-bit color display, e.g., for animation, is usually much slower than 8-bit indexed color displays. Some packages convert 24-bits to 8-bit indexed color for animation.
17. Animation of sections at 10–20 frames/s or faster will give an impression of smooth progression through the data. The viewer will start to benefit from persistance of vision where the retina carries the previous view as the next is seen. The brain, too, will aid this process by subconsiously linking cross-sections of objects seen in neighboring sections to give the impression of a continuous structure running through the volume ***(12)***. Features that cannot be seen clearly in a single section or montage can be more readily understood. It is important to ensure good lighting and a high contrast, good quality display to benefit from these visual perception processes.
18. When you play a smooth animation of this sequence the reconstruction will apear to rotate on the screen. Again, your eye and brain fills in the gaps between the

presented views, to enhance features that appear to move quickly round the periphery of the data volume, or more slowly toward the center of the data volume.

19. The purpose of the surface visualizations is to see the boundaries of all the cells and the way they are arranged in the tissue. This threshold technique uses a single value to pick out several objects in a volume and so you may have to use an average threshold for a group of cells. More sophisticated gradient boundary operators are offered by some packages that do not require a single threshold and can highlight both bright and darker objects in the same field. All the volume measurements presented here are done with thresholds on a cell by cell basis.
20. This first part of the visualisation uses one of the two-pass visualization modes of the Bio-Rad Lasersharp software. The distance on each side of the surface is entered as a use variable (typically 5–10 voxels each side).

Acknowledgments

This work was funded by The Wellcome Trust (R. J. E.). N. S. W. is a Royal Society Industry Fellow.

References

1. Hoffmann, E. K. and Simonsen, L. O. (1989) Membrane mechanisms In volume and pH regulation in vertebrate cells. *Physiol. Rev.* **69**, 315–382.
2. Hoffmann, E. K. and Dunham, P. B. (1995) Membrane mechanisms and intracellular signalling in cell volume regulation. *Int. Rev. Cytol.* **161,** 173–262.
3. Raat, N. J. H., de Smet, P., Van Driessche, W., Bindels, R. J. M. and van Os, C. H (1996). Measuring volume perturbation of proximal tubular cells in primary culture with three different methods. *Am. J. Physiol.* **271,** C235–C241.
4. Errington, R.J., Fricker, M.D., Wood, J.L., Hall, A.C. and White, N.S. (1997) Four-dimensional imaging of living chondrocytes in cartilage using confocal microscopy: a pragmatic approach. *Am. J. Physiol.* **272,** C1040–C1051.
5. White, N.S., Errington, R.J., Fricker, M.D., and Wood, J.L. (1996) Aberration control in quantitative imaging of botanical specimens by multi-dimensional fluorescence microscopy. *J. Microsc.* **181,** 99–116.
6. Beletsky, I. P. and Umansky, S. R. (1990) A new assay for cell death. *J. Immunol. Meth.* **134,** 201–205.
7. Ince, C., Ypey, D. L., Dieselhoff-den Dulk, M. C. C., Visser, J. A. M., De Vos, A. and van Furth, R. (1983) Micro-CO_2-incubator for use on a microscope. *J. Immunol. Methods* **60,** 269–275.
8. Terasaki, M. and Dailey, M.E. (1995). Confocal microscopy of living cells, in *Handbook of Biological Confocal Microscopy*, second edition (Pawley, J. B., ed.), pp. 327–344.
9. van Vliet, L. J. (1993) Grey-scale measurements in multi-dimensional digitised images. PhD thesis Delft University Press.

10. Shaw, P. J. (1998) Computational deblurring of fluorescence microscope images, in *Cell Biology A Laboratory Handbook*, second edition (Celis, J. E., ed.), pp. 206–218.
11. Guilak, F. (1993) Volume and surface area measurement of viable chondrocytes in situ using geometric modelling of serial confocal sections. *J. Microsc.* **173,** 245–256.
12. White, N. S. (1995) Visualisation systems for multidimensional CLSM images, in *Handbook of Biological Confocal Microscopy*, second edition (Pawley, J. B., ed.), pp. 211–254.